Title: Proinsulin attenuates the loss of vision and delays apoptosis of photoreceptors in a mouse model of retinitis pigmentosa.

Authors: Silvia Corrochano[1], Rima Barhoum[2], Patricia Boya[1], Ana I Arroba[1], Natalia Rodríguez-Muela[1], Violeta Gómez-Vicente[1], Fátima Bosch[3], Flora de Pablo[1], Pedro de la Villa[2] and Enrique J. de la Rosa[1,*].

Affiliations:

[1] 3D Lab (Development, Differentiation & Degeneration), Dept. of Cellular and Molecular Physiopathology, Centro de Investigaciones Biológicas, Consejo Superior de Investigaciones Científicas, C/ Ramiro de Maeztu 9, 28040 Madrid, Spain.

[2] Dept. of Physiology, Universidad de Alcalá, 28871 Alcalá de Henares, Spain.

[3] Dept. of Biochemistry and Molecular Biology, Center of Animal Biotechnology and Gene Therapy, Universitat Autònoma de Barcelona, 08193 Bellaterra, Spain.

* Corresponding Author: Enrique J. de la Rosa,

Centro de Investigaciones Biológicas, CSIC,

C/ Ramiro de Maeztu 9, 28040 Madrid, Spain.

E-mail: ejdelarosa@cib.csic.es

Phone: 34/918373112

Fax: 34/915349201

Grant information: This research was supported by grants from the Spanish Ministerio de Educación y Ciencia (SAF2001-1038, SAF2004-05870 and SAF2007-66175 to EJdlR and PdlV; BFU2004-02352 to FdP; SAF2005-01262 to FB), Spanish Ministerio de Sanidad y Consumo (RETIC RD-06 to FdP and FB), the Comunidad de Madrid (08.5-0019.1/2001 to EJdlR and 08.5-0049/2003 and CCG06-UAH/BIO-0711 to PdlV), Fundación Médica Mutua Madrileña (to EJdlR) and Fundaluce (to PdlV). SC and NRM were supported by a postgraduate fellowship from the Ministerio de Educación y Ciencia, PB by a Ramón y Cajal contract from the Ministerio de Educación y Ciencia, AIA by a postdoctoral contract from the Fondo de Investigaciones Sanitarias and VGV by an I3P postdoctoral contract from the European Social Fund.

Word count:

Title: 121 characters

Abstract: 233 words

Main text: 3229 words

Figures: 8, plus 2 supplementary

Abstract

PURPOSE: Retinitis pigmentosa (RP) is a heterogeneous group of inherited conditions that lead to blindness and for which there is no effective therapy. Apoptosis of photoreceptors is a common feature in animal models of the disease. Thus, we have studied the therapeutic potential of proinsulin, an anti-apoptotic molecule that is active during retinal development. METHODS: Transgenic mice expressing human proinsulin (hPi) in the skeletal muscle were generated in a mixed C57BL/6:SJL background and back-crossed to a C57BL/6 background. Two independent lineages of transgenic mice were established, in which hPi production in muscle was constitutive and not regulated by glucose levels. hPi levels in serum, muscle and retina were determined with a commercial ELISA kit, visual function was evaluated by electroretinogram (ERG) recording and programmed cell death was assessed by TUNEL. Immunohistochemistry was used to evaluate retinal structure preservation and oxidative damage. RESULTS: Transgenic expression of hPi in the rd10 retinal degeneration mouse model led to prolonged vision, as determined by ERG recording, in a manner that was related to the level of transgene expression. This attenuation of visual deterioration was correlated with a delay in photoreceptor apoptosis, as well as with the preservation of retinal cytoarchitecture, particularly that of the cones. CONCLUSIONS: Our results provide a new basis for possible therapies to counteract retinitis pigmentosa, as well as a new tool to dissect out the mechanisms involved in the progress of retinal neurodegeneration.

Introduction

Programmed cell death is a self-destructive physiological process essential for both, the correct development of an organism and its homeostasis [1]. Consequently, unregulated cell death underlies many diseases, including neurodegenerative disorders [2]. Thus, understanding how cell death is regulated during neural development may help to establish new therapeutic approaches to prevent neurodegeneration [3].

RP constitutes a large, heterogeneous group of inherited retinal neurodegenerative conditions that involve progressive loss of retinal function in parallel with the loss of photoreceptors through apoptosis [4-6]. Thus, attenuation of apoptosis represents good therapeutic target in RP, especially considering the vast heterogeneity of the disease [7]. The most extensively studied animal model of RP is the *rd1* mouse, which carries a recessive nonsense mutation in the *pde6b* gene. Indeed, a number of mutations have been found in the catalytic domain of the human *pde6b* gene in patients suffering from autosomal recessive RP [8, 9]. The *rd1* mouse is characterized by an early onset of photoreceptor loss, apoptosis peaking around postnatal day (P) 14-15 [4, 10]. As a consequence, ERG recordings of visual function never reach notable values, even in those cases where attenuation has been reported. A more recently characterized animal model, the *rd10* mouse, also carries a recessive mutation in the *pde6b* gene, which produces a delayed phenotype when compared to the *rd1* mouse. Therefore, ERGs can be readily obtained prior to degeneration in this model [11, 12]

and, accordingly, this situation better resembles the course of the human disease.

Molecules that promote survival, such as growth factors BDNF, CNTF, FGFs, GDNF, PEDF, are moderately successful in preventing disease progression when employed in animal models [13-18]. Antioxidants also provide modest protection, probably by reducing the oxidative damage found in the *rd1* mouse retinas [19, 20]. Members of the insulin family are well-characterized neuroprotective molecules active both in development and aging [21-23]. We have previously reported that locally expressed proinsulin acts as survival factor during embryonic retinal development in the chick and the mouse [24-27]. In the present study we show that transgenic human proinsulin expression in *rd10* mice attenuates retinal degeneration, as assessed by the maintenance of ERG and the histological preservation of photoreceptors. Systemic proinsulin was able to reach retinal tissue, delay apoptotic death of photoreceptors, and decrease oxidative damage. Thus, proinsulin represents a possible new therapy for RP, as well as a new tool to dissect out the mechanisms involved in pathological cell death.

Materials and Methods

Animals

All procedures were approved by the respective local ethics committee for animal experimentation, and experiments were carried out in accordance with the European Union guidelines and ARVO statement for use of animals in ophthalmic and vision research. Control wild type (wt) C57BL/6J mice were obtained from the Jackson Laboratory (Bar Harbor, ME). The mouse model of retinal degeneration, *pde6b*^{rd10} (*rd10*), also on a C57BL/6J background, was kindly provided by Dr. B. Chang (Jackson Laboratory).

Transgenic mice expressing human proinsulin (hPI) driven by the myosin light chain (MCL)-I promoter and a muscle-specific enhancer were generated on a mixed C57BL/6:SJL background and back-crossed to a C57BL/6 background. Two lines of transgenic mice (L1 and L2) were established in which hPi production in muscle was constitutive and not regulated by glucose levels. Expression of hPi in transgenic mice was confirmed by ELISA of muscle and serum samples, whereas hPi was undetectable in non-transgenic animals. Glucose levels in serum, as well as weight of transgenic mice in comparison with wt animals were followed over a period of 13 months (Supplementary Fig. 1).

The *rd10* mice used in this study were homozygous for the *pde6b*^{rd10} mutation, while the transgenic mice were either homozygous or hemizygous for the hPi transgene, as indicated.

The hPi genotype was determined by Southern blotting using specific dCT^{32}P labeled probes for hPi and for mouse S16 as a reference gene (Random Primer

Kit, Stratagene, La Jolla, CA), hybridized at the same time. Phosphorimager IP software (Fuji Film, Kanagawa, Japan) was used to quantify the signal corresponding to the respective specific bands, and the ratio between both bands was used to establish the zygosity of each transgenic animal.

The *rd10* genotypes were assessed as recommended by the Jackson Laboratory [11].

ERG recordings

Mice were dark-adapted overnight and subsequent manipulations and ERG recordings were performed in dim red light. Mice were anaesthetized with an intraperitoneal injection of a ketamine (95 mg/Kg) and xylazine (5 mg/Kg) solution and maintained on a heating pad at 37°C. Pupils were dilated by applying a topical drop of 1% tropicamide (Colircusí Tropicamida, Alcon Cusí, El Masnou, Barcelona, Spain). To optimize electrical recording, a topical drop of 2% Methocel (Ciba Vision, Hetlingen, Switzerland) was instilled on each eye immediately before situating the corneal electrode. Flash-induced ERG responses were recorded from the right eye in response to light stimuli produced with a Ganzfeld stimulator. The intensity of the light stimuli was measured with a photometer at the level of the eye (Mavo Monitor USB, Gossen, Nürenberg, Germany). At each light intensity, 4–64 consecutive stimuli were averaged with an interval between light flashes in scotopic conditions of 10 s for dim flashes and of up to 60 s for the highest intensity. In contrast, under photopic conditions the interval between light flashes was fixed at 1 s. The ERG signals were amplified and band filtered between 0.3 and 1000 Hz with a Grass amplifier

(CP511 AC amplifier, Grass Instruments, Quincy, MA). Electrical signals were digitized at 20 kHz with a Power Lab data acquisition board (AD Instruments, Chalgrove, UK). Bipolar recording was performed between an electrode fixed on a corneal lens (Burian-Allen electrode, Hansen Ophthalmic Development Lab, Coralville, IA) and a reference electrode located in the mouth, with a ground electrode located in the tail. Under dark adaptation, rod-mediated responses were recorded to light flashes ranging from -4 to -1.5 log $cd \cdot s \cdot m^{-2}$, while mixed rod- and cone-mediated responses were recorded in response to light flashes ranging from -1.5 to 1.5 log $cd \cdot s \cdot m^{-2}$. Oscillatory potentials (OP) were isolated using white flashes of 0.48 log $cd \cdot s \cdot m^{-2}$ in a recording frequency range of 100–10000 Hz., and cone-mediated responses to light flashes ranging from 0.5 to 2 log $cd \cdot s \cdot m^{-2}$ on a rod-saturating background of 30 $cd \cdot m^{-2}$ were recorded. Flicker responses (20 Hz) to light flashes of 1.5 log $cd \cdot s \cdot m^{-2}$ were also recorded on a rod-saturating background. The amplitudes of the a-wave and b-wave were measured off-line and the results averaged. Measurements were performed by an observer blind to the experimental condition of the animal.

Detection of transgenic proinsulin

Human proinsulin production in transgenic mice was determined both in serum and muscle using an ELISA kit (human total proinsulin ELISA kit, LINCO Research, St. Louis, MO) according to manufacturer's instructions. For serum determination, 20 μl of serum were assayed in duplicates. For muscle determination, quadriceps muscle were first dissected and homogenized in 50 mM Tris-HCl, pH 7.4, 100 mM NaCl, 0.1% (w/v) Triton X-100 buffer. Duplicates

containing 30 μg of protein, as determined by the BCA method (Pierce, Rockford, IL), were assayed. To determine the access of proinsulin to the retina, litters of P25 wt and *rd10* mice were subcutaneously injected with 5 μg of hPi (in 100 μl of phosphate-buffered saline; Sigma P-4672, St Louis, MI; or kindly provided by Eli-Lilly). Retinal extracts were prepared two hours later by dissecting and homogenizing one retina in 50 μl of the Tris-HCl buffer described above, and duplicates of 20 μl were assayed.

Cell death progression

Programmed cell death was determined by terminal deoxynucleotidyl transferase-mediated dUTP nick-end labeling (TUNEL). Mice of the indicated genotype and age were decapitated, their eyes enucleated and the retinas dissected out and flat-mounted onto nitrocellulose filter (Sartorius, Göttingen, Germany) photoreceptor layer side up. Retinas were then fixed in 4% (w/v) paraformaldehyde in 0.1 M phosphate buffer pH 7.4 at 4ºC overnight, and subsequently processed for TUNEL staining as described previously (Promega, Madison, WI; [27]). After labeling, the retinas were mounted in Vectashield containing DAPI (Vector laboratories, Burlingame, CA) and analyzed on a TCS SP2 Laser-confocal microscope (Leica, Microsystems, Wetzlar, Germany). Serial optical sections were acquired with a 10X objective every 5 μm in depth around the optic nerve head. To ensure that TUNEL-positive nuclei were located in the outer nuclear layer (ONL) the depth of analysis was set according to ONL thickness, as determined in retinal sections. The number of total TUNEL-positive cells per mm^2 was quantified in compiled projections from at least 4 retinas per

experimental group. The central retina area quantified represents approximately 15% of the retinal surface.

Histochemistry

Animals from the different experimental groups were decapitated, their eyes enucleated, immediately embedded in Tissue-Tek (Sakura Finetek, Torrance, CA), and frozen in dry ice. Sections of 12 μm were cut with a cryostat (Leica CM 1900, Leica Microsystems) and mounted on Poly-Lysine coated glass slides (Fisher Biotech, Pittsburgh, PA). Cryo-sections were then dried at room temperature, fixed for 15 min with 4% (w/v) paraformaldehyde in phosphate-buffered saline and stained with Alexa 488-conjugated peanut agglutinin (1:500, Molecular Probes, Eugene, OR) or a rabbit anti-acrolein antibody (1:150; AbD Serotec, Oxford, UK) followed by Alexa 488-conjugated goat anti-rabbit Igs (1:200; Molecular Probes). After staining, sections were mounted in Vectashield (Vector Laboratories) containing DAPI to counterstain the nuclei.

Results

Transgenic proinsulin expression preserves visual function in hPi/rd10 mice.

The anti-apoptotic activity of proinsulin during retinal development [25] prompted us to investigate a possible effect of proinsulin in the photoreceptor apoptosis associated to retinal degeneration. We crossed two hPi transgenic mice lineages (L1 and L2) with the retinal degeneration model *rd10* and analyzed the visual function of hPi/*rd10* homozygous animals. ERG provided a comprehensive evaluation of visual function, both in scotopic (night, rod selective) and photopic (day-light, cone selective) conditions. While ERG waves could be recorded prior to degeneration in the *rd10* mouse, as previously described [11, 12, 28], the ERG amplitudes diminished as retinal degeneration occurred and they became negligible by P30 (Fig. 1). By contrast, visual activity could still be measured at P30 in the two different hPi/*rd10* mice lines (Fig. 1) and it was most prominent in the cones, whose degeneration is secondary to that of rods [29]. Thus, transgenic expression of human proinsulin in muscle was able to attenuate the loss of vision in *rd10* mice.

The preservation of visual function in hPi/rd10 mice correlates with proinsulin levels.

We assessed the correlation between hPi expression levels and the preservation of visual function, a particularly relevant issue when contemplating the therapeutic potential of any factor. As such, we evaluated visual function by recording ERGs from both homozygous and hemizygous hPi/*rd10* animals of lineage 1. ERG responses were recorded at P30 in dark- and light-adapted

conditions to reflect rod- and cone-mediated vision, and standard ERG-wave amplitudes were determined. As a result, we identified significant differences in the averaged ERG amplitude values of b_{dim}, OP, a_{max}, b_{max}, b_{phot} and flicker responses in each experimental group (Fig. 2). Indeed, each of these ERG parameters was higher in homozygous hPi/*rd10* mice than in *rd10* mice ($p<0.001$) and, notably, the mean amplitude values of flicker, b_{phot} and OP were 60%, 37% and 26% of the respective values from wt mice. Furthermore, OP, a_{max}, and flicker values from hemizygous hPi/*rd10* animals were also significantly higher than those from *rd10* mice ($p<0.01$).

Once we had established a correlation between visual function preservation and transgenic hPi gene dosage, we examined the correlation between hPi protein levels and visual function. The measured hPi concentrations in serum were below 15 pM, close to the inferior limit of the hPi ELISA kit used for their determination. Since the hPi transgene was under the control of the MLC-I muscle promoter, we determined the levels of hPi produced in muscle instead. Significant correlation between muscle hPi protein and several ERG parameters was found. Indeed, there was a hyperbolic correlation between hPi muscle content and the amplitudes of b_{max}, OP, b_{phot} and flicker (Fig. 3). Therefore, a dose-response relationship between production of transgenic hPi in muscle and induced neuroprotection in the retina exists, which supports the potential therapeutic use of proinsulin.

In addition, we evaluated the duration of the neuroprotective effect and functional preservation afforded by proinsulin, by comparing ERGs from wt, *rd10* and

hPi/*rd10* animals up to P55 (Fig. 4, and Supplementary Fig. 2). The scotopic and photopic b-waves (b_{max} and b_{phot}) were partially preserved in hPi/*rd10* mice even at P55, a period of time that doubled the period of vision in this model (Fig. 4). Remarkably, cone function was better preserved and long-lasting than rod function. Together, these experiments demonstrate that sustained low levels of systemic proinsulin actually delay visual loss in *rd10* dystrophic animals.

Systemic proinsulin reaches the retinal tissue and delays photoreceptor cell death.

The effects of transgenic hPi reflected in the ERGs indicated that it acted directly or indirectly on retinal tissue, extending visual function. However, we were unable to detect hPi in retinal extracts from hPi/*rd10* mice. Thus, to assess whether or not systemic proinsulin did indeed reach the retinal tissue, we subcutaneously injected a single dose of hPi (5 μg) and 2 hours later determined proinsulin content in serum and retinal extracts. In this manner we could detect proinsulin in the retina and, interestingly, retinal levels roughly correlated with proinsulinemia (Fig. 5). Thus, the incapacity to detect proinsulin in hPi/*rd10* retinas probably reflects the very low amounts of proinsulin produced or accumulated by the animals, which nevertheless were sufficient to attenuate the loss of vision.

The loss of visual function in *rd10* mice is associated to massive loss of photoreceptors in the outer nuclear layer (ONL) [11, 12, 28]. Since we observed attenuation of vision loss in transgenic hPi/*rd10* animals, we investigated whether proinsulin expression was able to specifically interfere with photoreceptor apoptosis. Cell death, visualized by TUNEL staining of whole-mount retinas, was

delayed in hPi/*rd10* when compared to *rd10* mice (Fig. 6), an observation that paralleled the delay in the loss of visual function already described (Fig. 4). Therefore, systemic proinsulin was able to exert an anti-apoptotic effect on photoreceptors.

Transgenic proinsulin preserves retinal structure and decreases oxidative damage.

We further examined the histopathological aspects of the *rd10* mouse retina in comparison with hPi/*rd10*. In agreement with our previous observations, transgenic hPi/*rd10* animals displayed more photoreceptor rows than *rd10* animals at P32 (Fig. 7). This histological feature also correlated with transgene dosage, as described for the ERG (Fig. 2), as well as with proinsulinemia. Cone preservation was studied in more detail by staining the retina with the specific peanut agglutinin cone marker, which labels cone outer segments as well as synaptic terminals. A remarkable preservation of these cells was observed in hPi/*rd10* retinas, sustaining the ERG cone responses described in Fig. 4.

Increased lipid oxidation has been demonstrated in the retinas of *rd1* and *rd10* mouse models [19, 30] and oxidative damage appears to trigger cell death in both, physiological and pathological conditions [31, 32]. Thus, we determined whether proinsulin might interfere at this level of the neurodegenerative process. There was strong immunoreactivity for acrolein, a product of lipid oxidation, in the *rd10* mouse retina (Fig. 8), in accordance with previous observations of Komeima and collaborators [30]. Interestingly, the immunoreactivity for acrolein was much weaker in hPi/*rd10* transgenic animals than in *rd10* at P32, suggesting that the

prevention of oxidative damage may be one of the primary effects of proinsulin (Fig. 8).

Discussion

Together our results show that proinsulin preserves photoreceptor number and structure, as well as visual function in the degenerating *rd10* mouse retina, fulfilling anti-apoptotic and anti-oxidant roles. Partial preservation of visual function in ERGs has been achieved by treatment with certain survival molecules, such as GDNF in the transgenic S334ter-4 rat [17], BDNF in the rhodopsin mutant mouse [18], and antioxidants in the *rd1* mouse [19]. Nevertheless, the preservation of ERG amplitudes reported in those studies is much lower than that observed here with proinsulin. Since different animal models and delivery methods have been employed, we can only claim at the present that proinsulin displays a promising neuroprotective effect.

Another interesting difference of the approach adopted here is the effectiveness of systemic delivery. Most experimental treatments for RP involve direct retinal delivery by viral transfer [16, 17] retinal transgene expression [18], or by using intravitreal encapsulated cells [33]. However, systemic administration of antioxidants has also been shown to provoke a modest neuroprotective effect [19, 30]. Although systemic delivery would perhaps not be the primary choice in retinal therapy, this aspect raises new questions about the biological availability of proinsulin and other members of this family in nervous tissue and their utility in neuroprotective therapies. Indeed, systemic IGF-I seems to be able to pass the blood-brain barrier and induce neuroprotection [34].

We have found a hyperbolic correlation between the amount of proinsulin expressed in the muscle, where the transgene is transcriptionally active, and the

preservation of visual function parameters. This correlation is reminiscent of a receptor-mediated effect of proinsulin. Proinsulin has only weak affinity for the classic insulin-receptor and it has a poor metabolic potential (5-10 % of that of insulin; [35]), which was reflected by the fact that all animals remained in the normal glycaemic and weight range (Supplementary Fig.1 and data not shown). An atypical, hybrid insulin/IGF-I receptor is present in the developing retina when proinsulin exerts its survival role with similar efficiency to insulin or IGF-I [27, 36]. Proinsulin seems to block developmental cell death at various levels, including activation of PI3K/Akt and ERK pathways, stimulation of prosurvival chaperones, as well as interference with caspases and cathepsins [27, 37-40]. This pleiotropic effect may underlie its neuroprotective action throughout blocking the multiple death pathways described in the rd muse models. To determine whether or not proinsulin survival pathways coincide under physiological and pathological conditions requires further studies.

Cell death and visual loss still occur and eventually led to blindness in hPi/*rd10* mice. However, proinsulin provides an extended window of visual function, especially with respect to day-light vision, which may be a useful therapeutic approach to ameliorate the dramatic impact of RP in human patients.

FIGURE LEGENDS

Figure 1.- ERG demonstrates the preservation of visual function in hPi/*rd10* mice. ERG's were obtained from wt, *rd10* and hPi/*rd10* mice at P30. Examples from two different hPi/*rd10* lineages (L1, L2) are shown. Rod and mixed responses were recorded under scotopic conditions to light flashes of -2.0 log $cd \cdot s \cdot m^{-2}$ and 1.5 log $cd \cdot s \cdot m^{-2}$, respectively. Cone-mediated responses were recorded to light flashes of 1.5 log $cd \cdot s \cdot m^{-2}$ on a rod saturating background of 30 $cd \cdot m^{-2}$. Standard ERG wave amplitudes are indicated in the wt mice panels for identification. The amplitudes of ERG recordings in the two hPi/*rd10* animal lineages were higher than in *rd10* animals. The same amplitude and time calibration are displayed for all recording traces.

Figure 2.- Preservation of ERG wave amplitudes in hPi/*rd10* mice correlates with hPi gene dosage. ERG wave amplitudes (b_{dim}, OP, a_{max}, b_{max}, b_{phot}, flicker; see Fig. 1) were quantified in wt, *rd10*, hemizygous (hemi hPi/*rd10*) and homozygous (homo hPi/*rd10*) mice at P30. Each circle represents a single animal. A non-parametric Kruskall-Wallis analysis was performed on all groups and significant differences were found for all variables ($p<0.001$). Non-parametric Mann-Whitney analysis showed significant differences between wt animals and *rd10*, hemi hPi/*rd10* and homo hPi/*rd10* (*a*, $p<0.001$; *a'*, no differences wt *vs.* homo hPi/*rd10*). Differences between homozygous hPi/*rd10* and *rd10* were significant for all values (*b*, $p<0.001$). Differences between the hemizygous hPi/*rd10* and *rd10* were significant for values of a_{max}, OP, and flicker (*c*, $p<0.005$).

Figure 3.- Preservation of ERG wave amplitudes in hPi/*rd10* mice correlates with proinsulin levels in muscle. ERG wave amplitudes for b_{max}, OP, b_{phot} and flicker are represented as a function of muscular proinsulin levels measured at P32. Each circle represents a single animal. A parametric Pearson test was performed and a significant hyperbolic correlation was found for b_{max} (r^2=0.455, n=16, p<0.005), OP (r^2=0.612, n=9, p<0.05), b_{phot} (r^2=0.504, n=16, p<0.005) and flicker (r^2=0.498, n=13, p<0.01).

Figure 4.- Visual function in hPi/*rd10* mice is maintained longer than in *rd10* mice. ERG wave amplitudes were quantified in wt, *rd10* and hPi/*rd10* at the ages indicated and average values for b_{max} and b_{phot} are shown (mean ± SEM, n= 4). Note that ERG waves in hPi/*rd10* mice decay slower than in *rd10* mice and that statistical significant differences were found (*a*, p<0.05; Kruskal-Wallis non-parametric ANOVA; n.s., non-significant).

Figure 5.- Systemic hPi is able to reach the retinal tissue. Litters of wt (closed circles) and *rd10* mice (open circles) were subcutaneously injected at P25 with 5 µg of hPi or vehicle (crosses). Proinsulin concentration was determined 2 hours later in serum and retinal extracts. Each symbol represents a single animal and proinsulin levels in the retinal tissue are represented as a function of proinsulinemia. Non-parametric Spearman Rho correlation with proinsulin injected mice (n=9) rendered rho=0.669 and p<0.05.

Figure 6.- Photoreceptor cell death is delayed in hPi/*rd10* mice. Cell death was determined by TUNEL in whole-mount retinas of *rd10* and hPi/*rd10* mice at the ages indicated. Representative labeled retinas are shown at P25 (A and B). The total number of TUNEL-positive nuclei was quantified in confocal images of equivalent central retina fields, as those shown in A and B, from at least 4 retinas per experimental group and represented in (C).

Figure 7.- Preservation of retinal structure in hPi/*rd10* mice. Retinal sections from wt, *rd10* and hPi/*rd10* mice at P32 were stained with DAPI (blue) to reveal retinal cytoarchitecture and with Alexa488-peanut agglutinin (green) to visualize the state of cones. Preservation of photoreceptor rows (vertical bars), as well as preservation of cone outer segments (upper arrowhead) and synaptic terminals (lower arrowhead), correlate with proinsulin gene dosage, as well as with proinsulinemia (1.3 pM in the shown hemizygous; 2.4 pM in the shown heterozygous). Retinal layers are labeled: outer nuclear layer (ONL), inner nuclear layer (INL) and ganglion cell layer (GCL). Scale bar, 25 µm.

Figure 8.- Reduction of lipid oxidation in hPi/*rd10* mice. Retinal sections from wt, *rd10* and hPi/*rd10* mice at P32 were stained with DAPI (blue) to reveal retinal cytoarchitecture and with anti-acrolein antibody (green) to visualize oxidative damage. The increased lipid oxidation observed in *rd10* retina is markedly reduced in hPi/*rd10* animals. Retinal layers are labeled: outer nuclear layer (ONL), inner nuclear layer (INL) and ganglion cell layer (GCL). Scale bar, 25 µm.

Supplemental material

Figure S1.- Variations in glucose levels and weight in hPi transgenic mice. Paired groups of C57BL/6J and hPi transgenic mice were employed to determine the evolution of glucose levels and weight over time. The animals were weighed monthly over a 13-month period (Gram Precision GM-100, Gram Precision, L'Hospitalet de Llobregat, Spain) and after each weighing, the food was removed from the cage and 18 hours later a blood sample was taken to determine glycaemia (Roche Accu-Chek Sensor, Roche Diagnostic, Mannheim, Germany). Mean values (± SEM) are shown.

Figure S2.- Visual function in hPi/rd10 mice is maintained for longer than in the

rd10 animals. Mixed and cone responses were recorded in wt, rd10 and hPi/rd10 animals with respect to light flashes of 1.5 log cd·s·m-2 on postnatal day 25, 35, 45 and 55 (indicated at the top of the recording traces). The complete disappearance of the ERG waves was observed in the rd10 control animals by p35 whereas in the hPi/rd10 animals, the ERG responses persisted even at P55.

References

1. Danial NN, Korsmeyer SJ. Cell death: critical control points. *Cell* 2004;116:205-219.
2. Mattson MP. Apoptosis in neurodegenerative disorders. *Nature reviews* 2000;1:120-129.
3. Nicholson DW. From bench to clinic with apoptosis-based therapeutic agents. *Nature* 2000;407:810-816.
4. Chang GQ, Hao Y, Wong F. Apoptosis: final common pathway of photoreceptor death in rd, rds, and rhodopsin mutant mice. *Neuron* 1993;11:595-605.
5. Farber DB, Flannery JG, Bowes-Rickman C. The rd mouse story: Seventy years of research on an animal model of inherited retinal degeneration. *Progress in Retinal and Eye Research* 1994;13:31-64.
6. Farrar GJ, Kenna PF, Humphries P. On the genetics of retinitis pigmentosa and on mutation-independent approaches to therapeutic intervention. *The EMBO journal* 2002;21:857-864.
7. Doonan F, Cotter TG. Apoptosis: a potential therapeutic target for retinal degenerations. *Current neurovascular research* 2004;1:41-53.
8. McLaughlin ME, Ehrhart TL, Berson EL, Dryja TP. Mutation spectrum of the gene encoding the beta subunit of rod phosphodiesterase among patients with autosomal recessive retinitis pigmentosa. *Proceedings of the National Academy of Sciences of the United States of America* 1995;92:3249-3253.
9. McLaughlin ME, Sandberg MA, Berson EL, Dryja TP. Recessive mutations in the gene encoding the beta-subunit of rod phosphodiesterase in patients with retinitis pigmentosa. *Nature genetics* 1993;4:130-134.
10. Portera-Cailliau C, Sung CH, Nathans J, Adler R. Apoptotic photoreceptor cell death in mouse models of retinitis pigmentosa. *Proceedings of the National Academy of Sciences of the United States of America* 1994;91:974-978.
11. Chang B, Hawes NL, Pardue MT, et al. Two mouse retinal degenerations caused by missense mutations in the beta-subunit of rod cGMP phosphodiesterase gene. *Vision research* 2007;47:624-633.
12. Gargini C, Terzibasi E, Mazzoni F, Strettoi E. Retinal organization in the retinal degeneration 10 (rd10) mutant mouse: a morphological and ERG study. *The Journal of comparative neurology* 2007;500:222-238.
13. Cayouette M, Behn D, Sendtner M, Lachapelle P, Gravel C. Intraocular gene transfer of ciliary neurotrophic factor prevents death and increases responsiveness of rod photoreceptors in the retinal degeneration slow mouse. *J Neurosci* 1998;18:9282-9293.
14. Cayouette M, Smith SB, Becerra SP, Gravel C. Pigment epithelium-derived factor delays the death of photoreceptors in mouse models of inherited retinal degenerations. *Neurobiology of disease* 1999;6:523-532.
15. Chong NH, Alexander RA, Waters L, Barnett KC, Bird AC, Luthert PJ. Repeated injections of a ciliary neurotrophic factor analogue leading to long-term photoreceptor survival in hereditary retinal degeneration. *Investigative ophthalmology & visual science* 1999;40:1298-1305.

16. Green ES, Rendahl KG, Zhou S, et al. Two animal models of retinal degeneration are rescued by recombinant adeno-associated virus-mediated production of FGF-5 and FGF-18. *Mol Ther* 2001;3:507-515.
17. McGee Sanftner LH, Abel H, Hauswirth WW, Flannery JG. Glial cell line derived neurotrophic factor delays photoreceptor degeneration in a transgenic rat model of retinitis pigmentosa. *Mol Ther* 2001;4:622-629.
18. Okoye G, Zimmer J, Sung J, et al. Increased expression of brain-derived neurotrophic factor preserves retinal function and slows cell death from rhodopsin mutation or oxidative damage. *J Neurosci* 2003;23:4164-4172.
19. Komeima K, Rogers BS, Lu L, Campochiaro PA. Antioxidants reduce cone cell death in a model of retinitis pigmentosa. *Proceedings of the National Academy of Sciences of the United States of America* 2006;103:11300-11305.
20. Ahuja P, Caffe AR, Ahuja S, Ekstrom P, van Veen T. Decreased glutathione transferase levels in rd1/rd1 mouse retina: replenishment protects photoreceptors in retinal explants. *Neuroscience* 2005;131:935-943.
21. de Pablo F, de la Rosa EJ. The developing CNS: a scenario for the action of proinsulin, insulin and insulin-like growth factors. *Trends in neurosciences* 1995;18:143-150.
22. Anlar B, Sullivan KA, Feldman EL. Insulin-like growth factor-I and central nervous system development. *Hormone and metabolic research Hormon- und Stoffwechselforschung* 1999;31:120-125.
23. Varela-Nieto I, de la Rosa EJ, Valenciano AI, Leon Y. Cell death in the nervous system: lessons from insulin and insulin-like growth factors. *Molecular neurobiology* 2003;28:23-50.
24. Hernandez-Sanchez C, Lopez-Carranza A, Alarcon C, de La Rosa EJ, de Pablo F. Autocrine/paracrine role of insulin-related growth factors in neurogenesis: local expression and effects on cell proliferation and differentiation in retina. *Proceedings of the National Academy of Sciences of the United States of America* 1995;92:9834-9838.
25. Diaz B, Serna J, De Pablo F, de la Rosa EJ. In vivo regulation of cell death by embryonic (pro)insulin and the insulin receptor during early retinal neurogenesis. *Development (Cambridge, England)* 2000;127:1641-1649.
26. Duenker N, Valenciano AI, Franke A, et al. Balance of pro-apoptotic transforming growth factor-beta and anti-apoptotic insulin effects in the control of cell death in the postnatal mouse retina. *The European journal of neuroscience* 2005;22:28-38.
27. Valenciano AI, Corrochano S, de Pablo F, de la Villa P, de la Rosa EJ. Proinsulin/insulin is synthesized locally and prevents caspase- and cathepsin-mediated cell death in the embryonic mouse retina. *Journal of neurochemistry* 2006;99:524-536.
28. Chang B, Hawes NL, Hurd RE, Davisson MT, Nusinowitz S, Heckenlively JR. Retinal degeneration mutants in the mouse. *Vision research* 2002;42:517-525.
29. Sahel JA, Mohand-Said S, Leveillard T, Hicks D, Picaud S, Dreyfus H. Rod-cone interdependence: implications for therapy of photoreceptor cell diseases. *Progress in brain research* 2001;131:649-661.

30. Komeima K, Rogers BS, Campochiaro PA. Antioxidants slow photoreceptor cell death in mouse models of retinitis pigmentosa. *Journal of cellular physiology* 2007;213:809-815.
31. Filomeni G, Ciriolo MR. Redox control of apoptosis: an update. *Antioxidants & redox signaling* 2006;8:2187-2192.
32. Valko M, Leibfritz D, Moncol J, Cronin MT, Mazur M, Telser J. Free radicals and antioxidants in normal physiological functions and human disease. *The international journal of biochemistry & cell biology* 2007;39:44-84.
33. Sieving PA, Caruso RC, Tao W, et al. Ciliary neurotrophic factor (CNTF) for human retinal degeneration: phase I trial of CNTF delivered by encapsulated cell intraocular implants. *Proceedings of the National Academy of Sciences of the United States of America* 2006;103:3896-3901.
34. Carro E, Trejo JL, Gomez-Isla T, LeRoith D, Torres-Aleman I. Serum insulin-like growth factor I regulates brain amyloid-beta levels. *Nature medicine* 2002;8:1390-1397.
35. King GL, Kahn CR. Non-parallel evolution of metabolic and growth-promoting functions of insulin. *Nature* 1981;292:644-646.
36. Garcia-de Lacoba M, Alarcon C, de la Rosa EJ, de Pablo F. Insulin/insulin-like growth factor-I hybrid receptors with high affinity for insulin are developmentally regulated during neurogenesis. *Endocrinology* 1999;140:233-243.
37. de la Rosa EJ, Vega-Nunez E, Morales AV, Serna J, Rubio E, de Pablo F. Modulation of the chaperone heat shock cognate 70 by embryonic (pro)insulin correlates with prevention of apoptosis. *Proceedings of the National Academy of Sciences of the United States of America* 1998;95:9950-9955.
38. Diaz B, Pimentel B, de Pablo F, de La Rosa EJ. Apoptotic cell death of proliferating neuroepithelial cells in the embryonic retina is prevented by insulin. *The European journal of neuroscience* 1999;11:1624-1632.
39. Rubio E, Valenciano AI, Segundo C, Sanchez N, de Pablo F, de la Rosa EJ. Programmed cell death in the neurulating embryo is prevented by the chaperone heat shock cognate 70. *The European journal of neuroscience* 2002;15:1646-1654.
40. Chavarria T, Valenciano AI, Mayordomo R, et al. Differential, age-dependent MEK-ERK and PI3K-Akt activation by insulin acting as a survival factor during embryonic retinal development. *Developmental neurobiology* 2007;67:1777-1788.

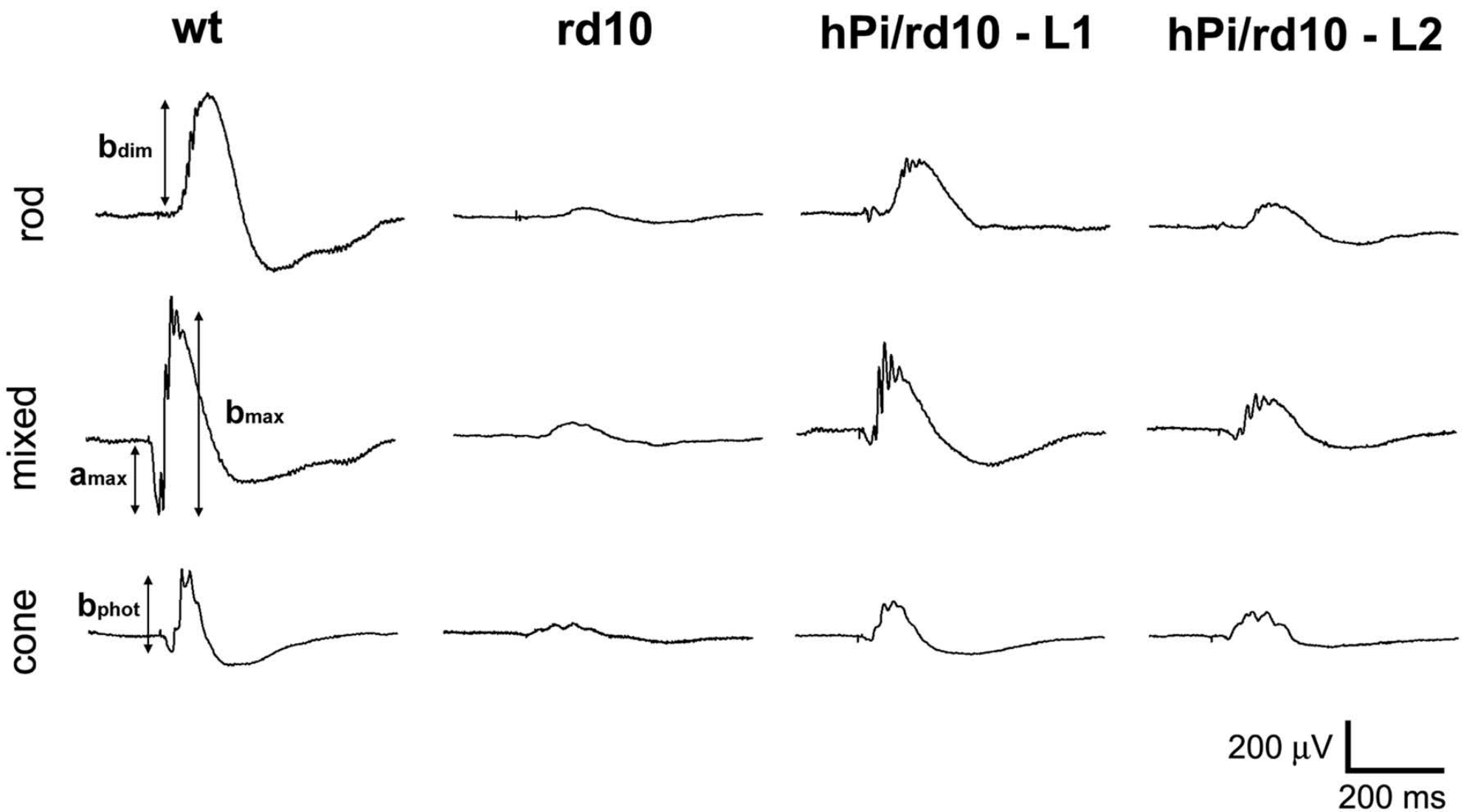
wt
rd10
hPi/rd10 - L1
hPi/rd10 - L2
rod
mixed
cone
bdim
bmax
amax
bphot
200 µV
200 ms

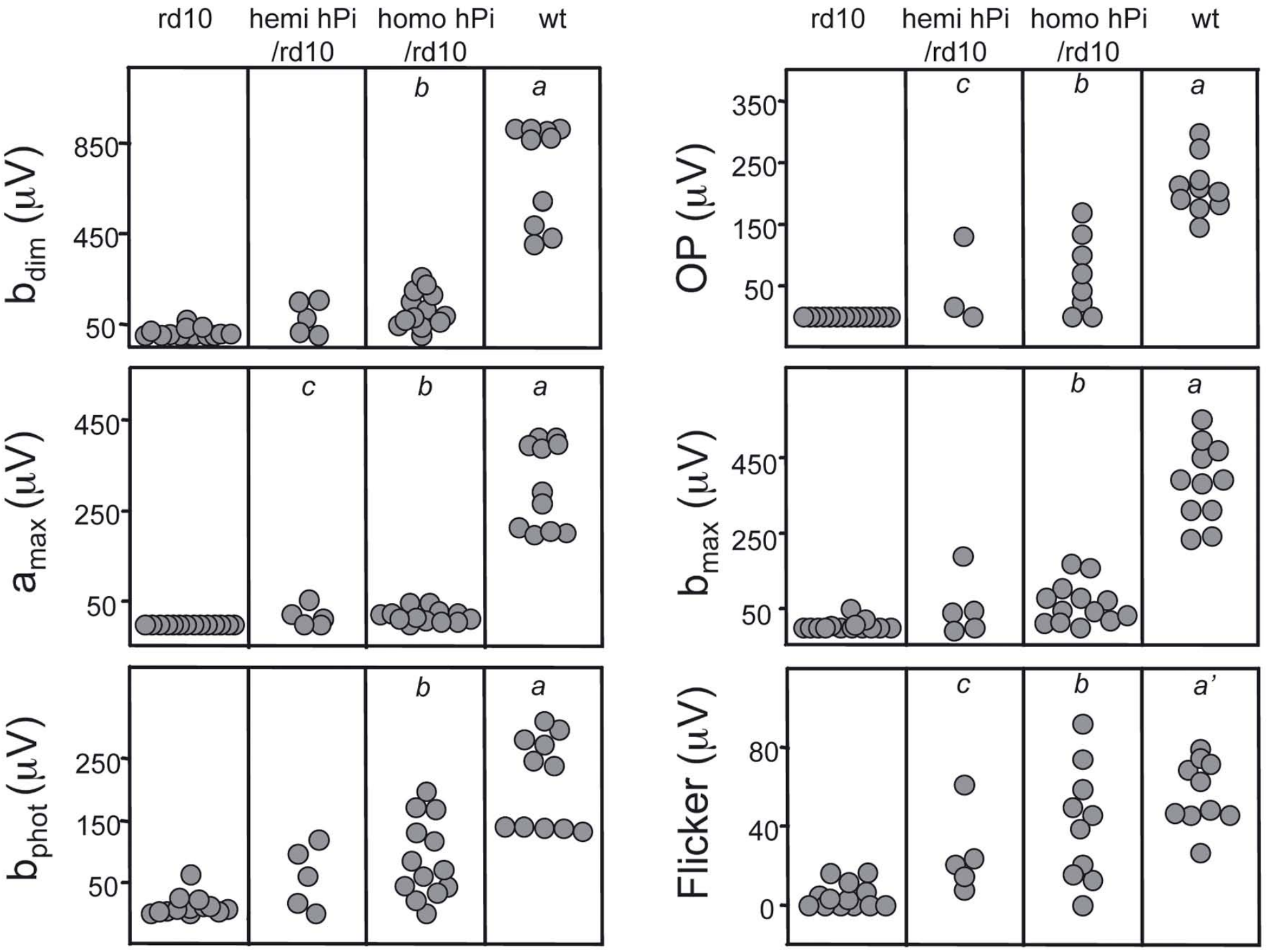
rd10
hemi hPi /rd10
homo hPi /rd10
wt
b_dim (µV)
850
450
50
b
a
OP (µV)
350
250
150
50
c
b
a
a_max (µV)
450
250
50
c
b
a
b_max (µV)
450
250
50
b
a
b_phot (µV)
250
150
50
b
a
Flicker (µV)
80
40
0
c
b
a'

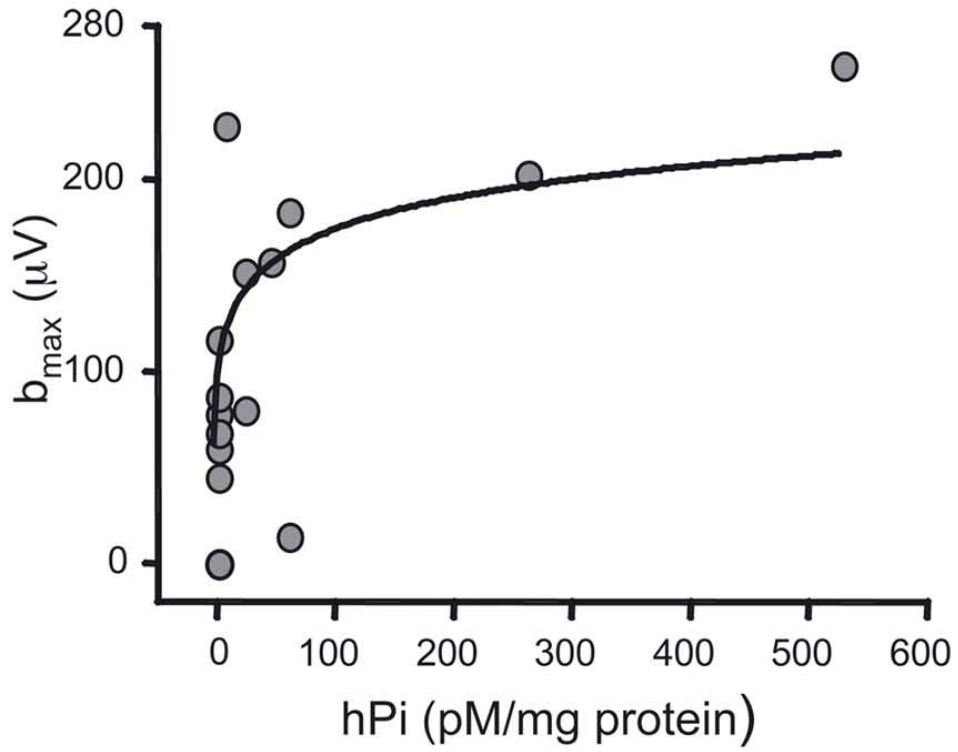
280
200
100
0
b_{max} (μV)
0
100
200
300
400
500
600
hPi (pM/mg protein)

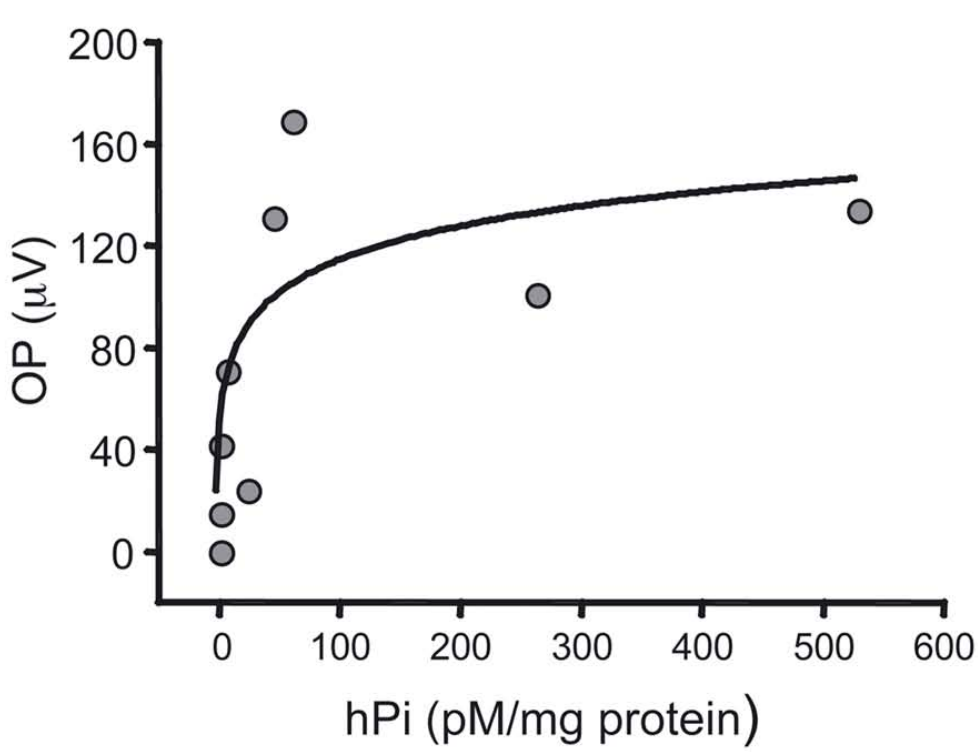
200
160
120
80
40
0
OP (μV)
0
100
200
300
400
500
600
hPi (pM/mg protein)

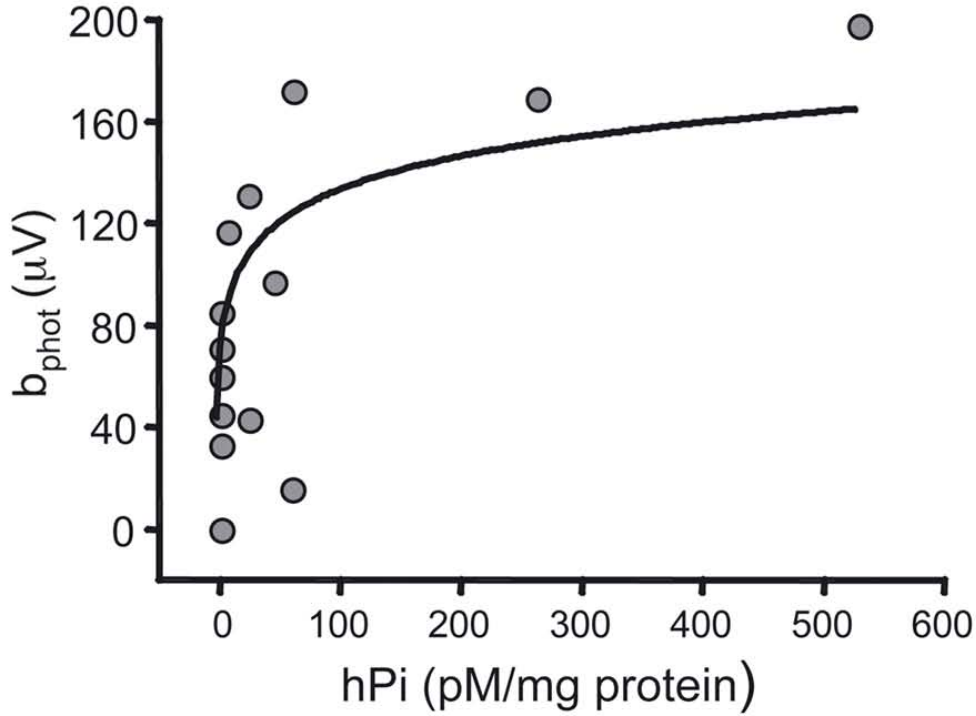
200
160
120
80
40
0
b_{phot} (μV)
0
100
200
300
400
500
600
hPi (pM/mg protein)

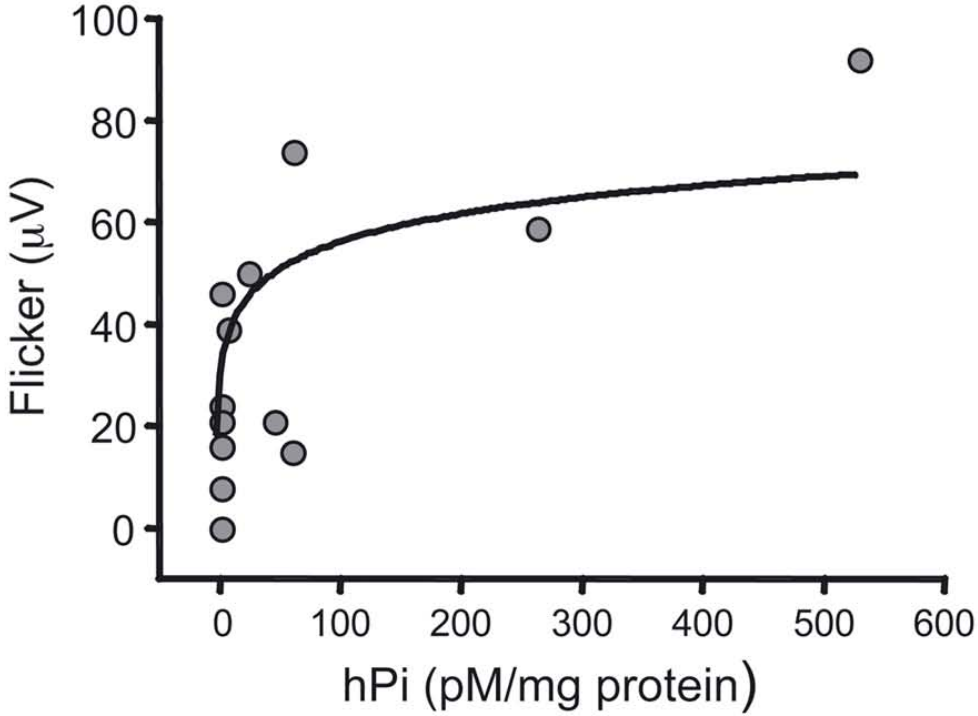
100
80
60
40
20
0
Flicker (μV)
0
100
200
300
400
500
600
hPi (pM/mg protein)

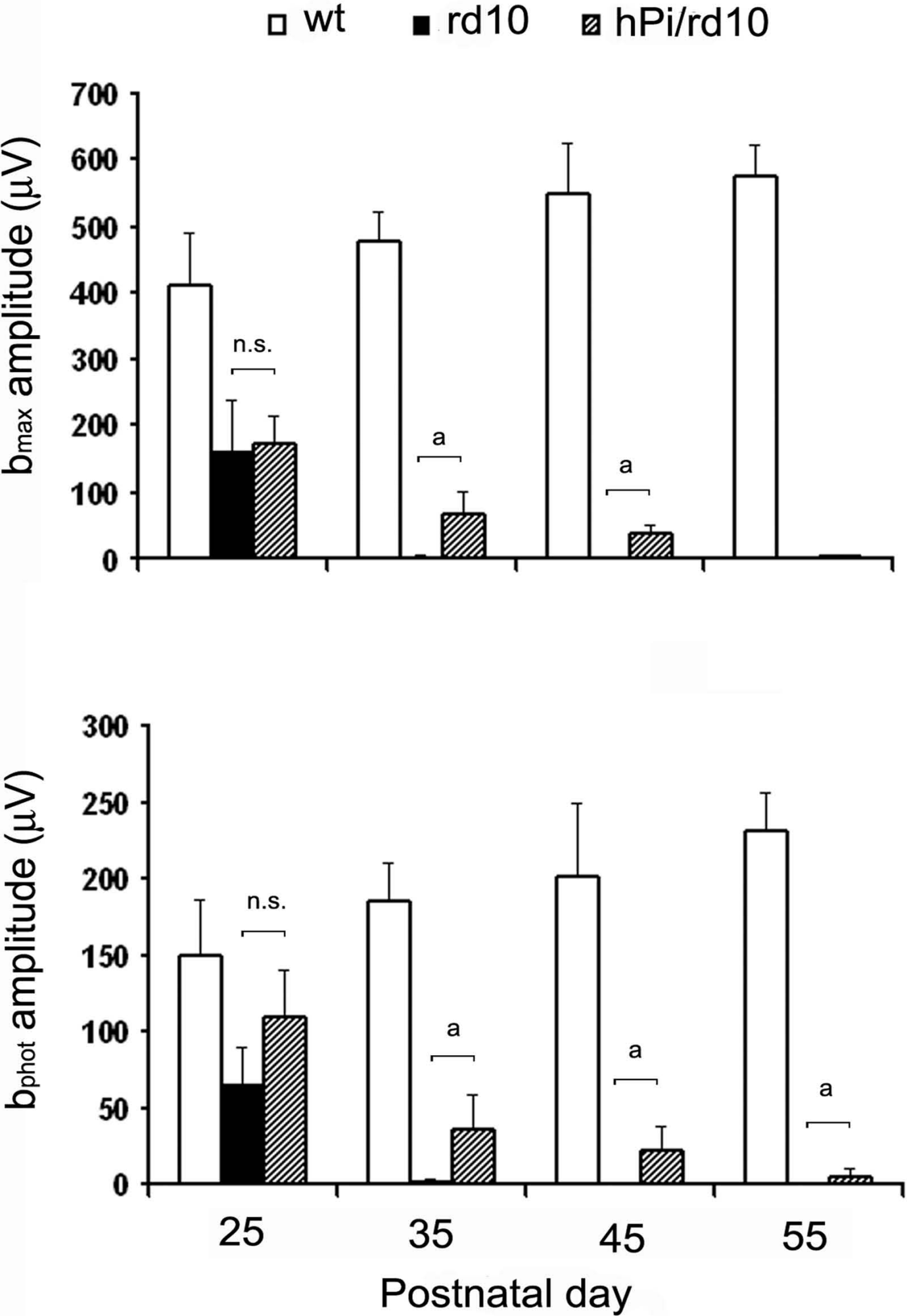
wt
rd10
hPi/rd10
b_{max} amplitude (μV)
700
600
500
400
300
200
100
0
n.s.
a
a
b_{phot} amplitude (μV)
300
250
200
150
100
50
0
n.s.
a
a
a
25
35
45
55
Postnatal day

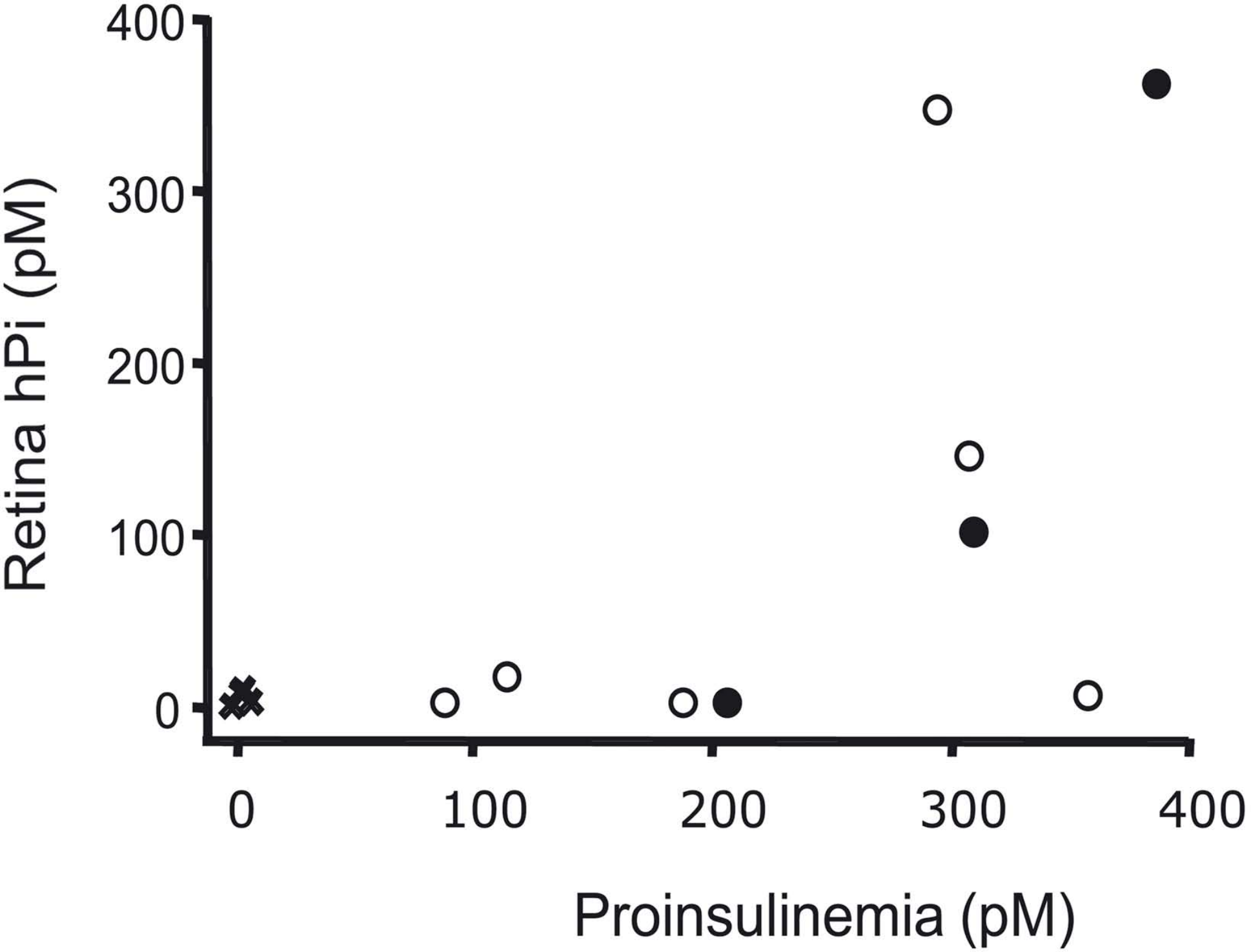
400
300
200
100
0
Retina hPi (pM)
0
100
200
300
400
Proinsulinemia (pM)

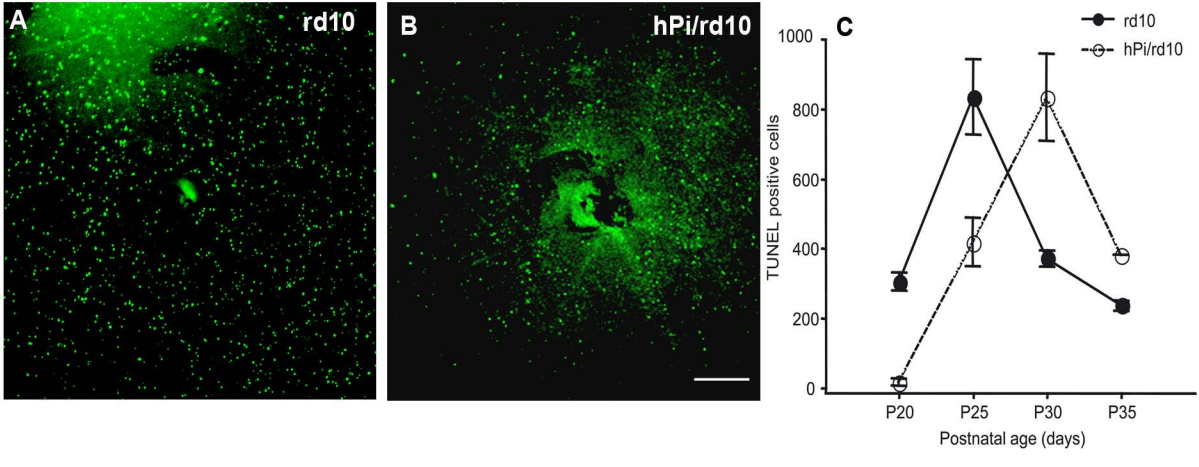
A
rd10
B
hPi/rd10
C
rd10
hPi/rd10
TUNEL positive cells
1000
800
600
400
200
0
P20
P25
P30
P35
Postnatal age (days)

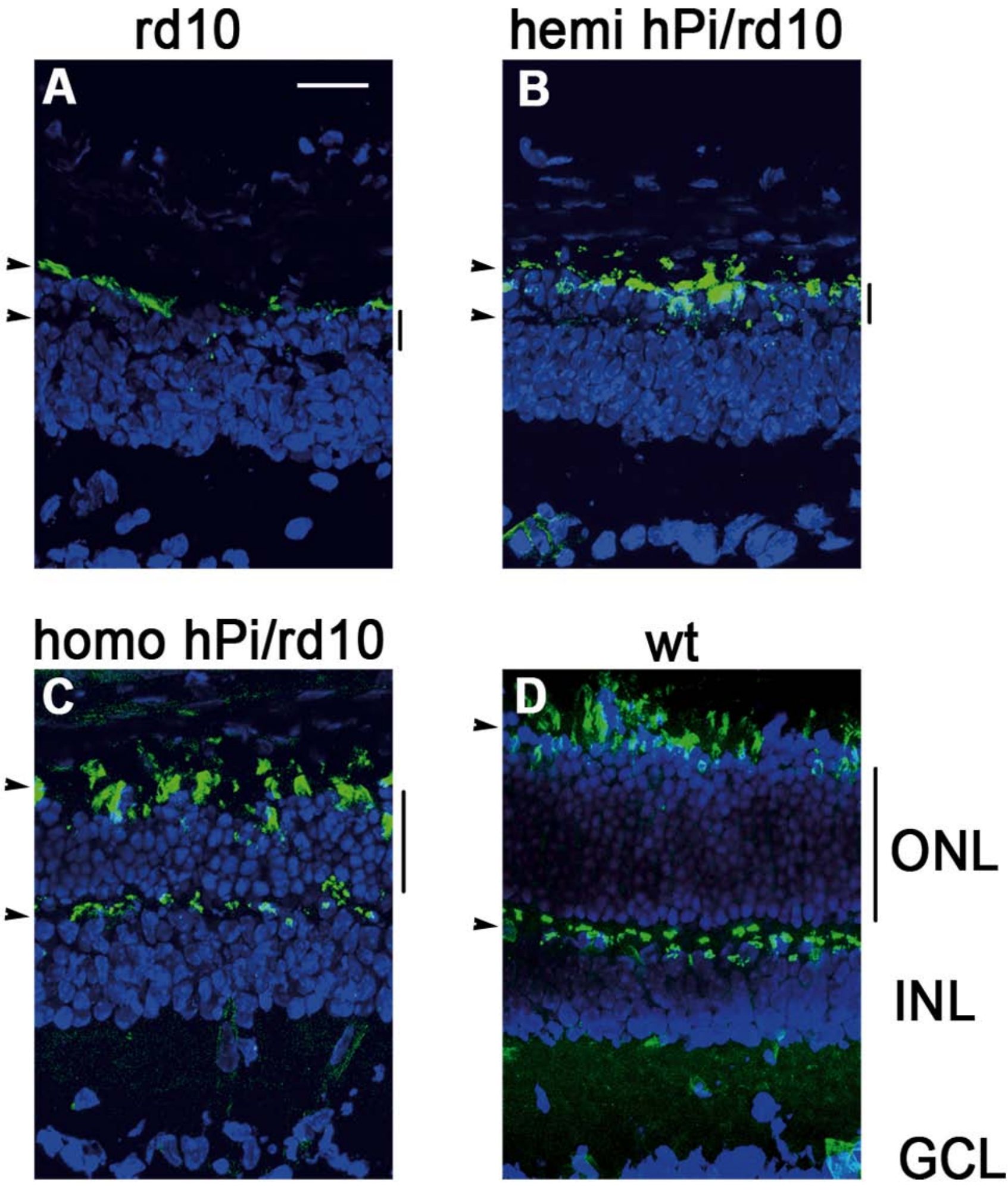
rd10
A
hemi hPi/rd10
B
homo hPi/rd10
C
wt
D
ONL
INL
GCL

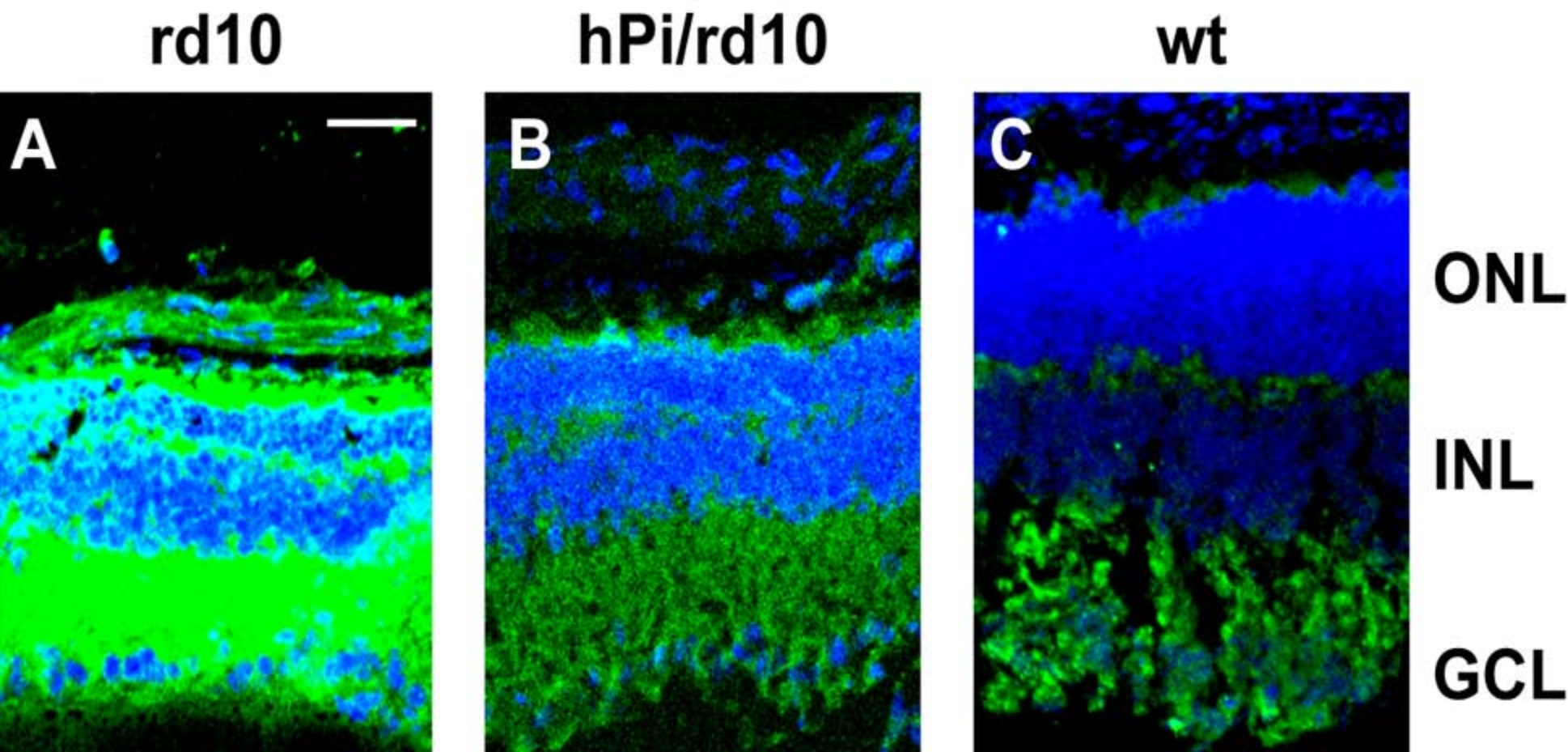
rd10
hPi/rd10
wt
A
B
C
ONL
INL
GCL

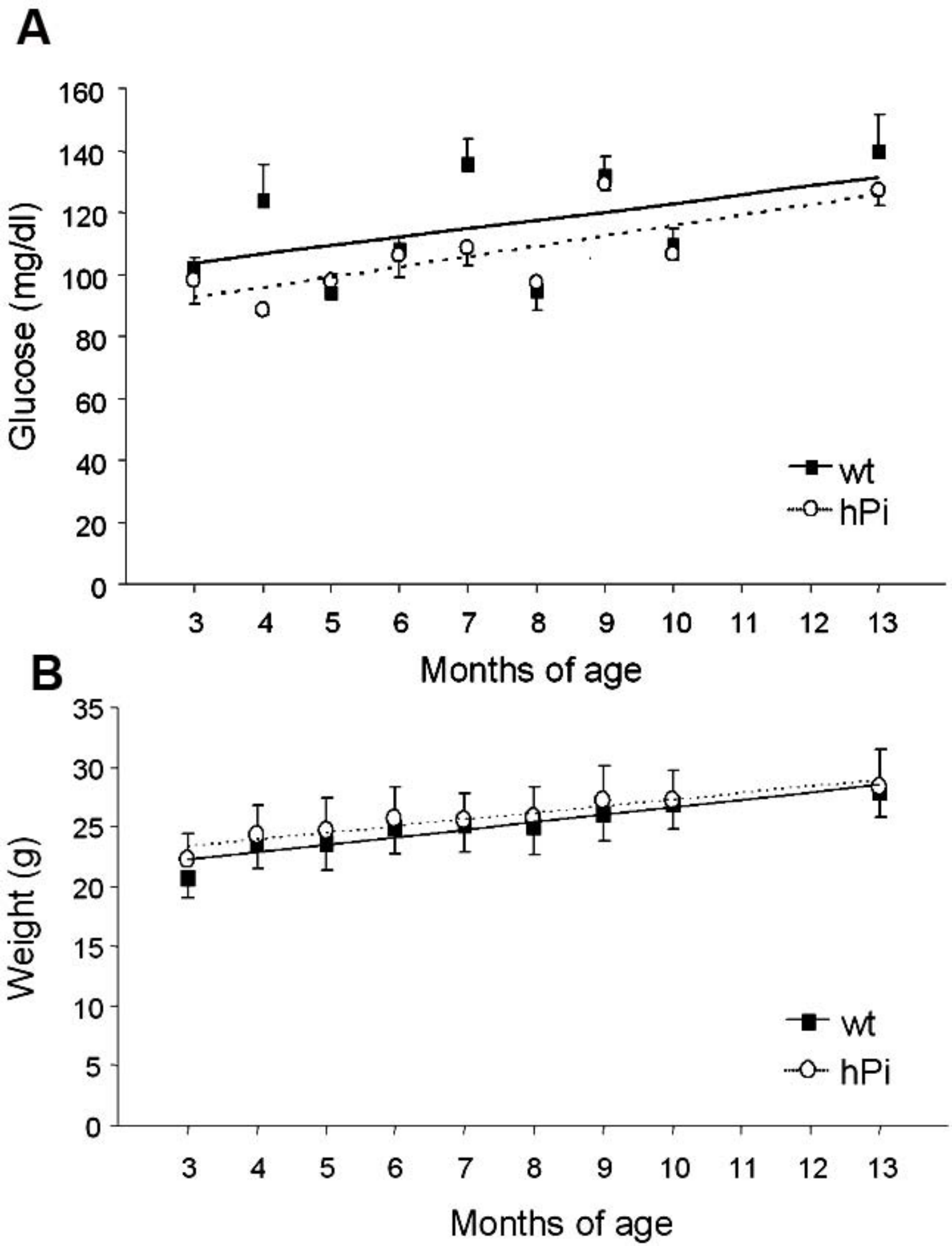
A
160
140
120
100
80
60
40
20
0
Glucose (mg/dl)
wt
hPi
3
4
5
6
7
8
9
10
11
12
13
Months of age
B
35
30
25
20
15
10
5
0
Weight (g)
wt
hPi
3
4
5
6
7
8
9
10
11
12
13
Months of age

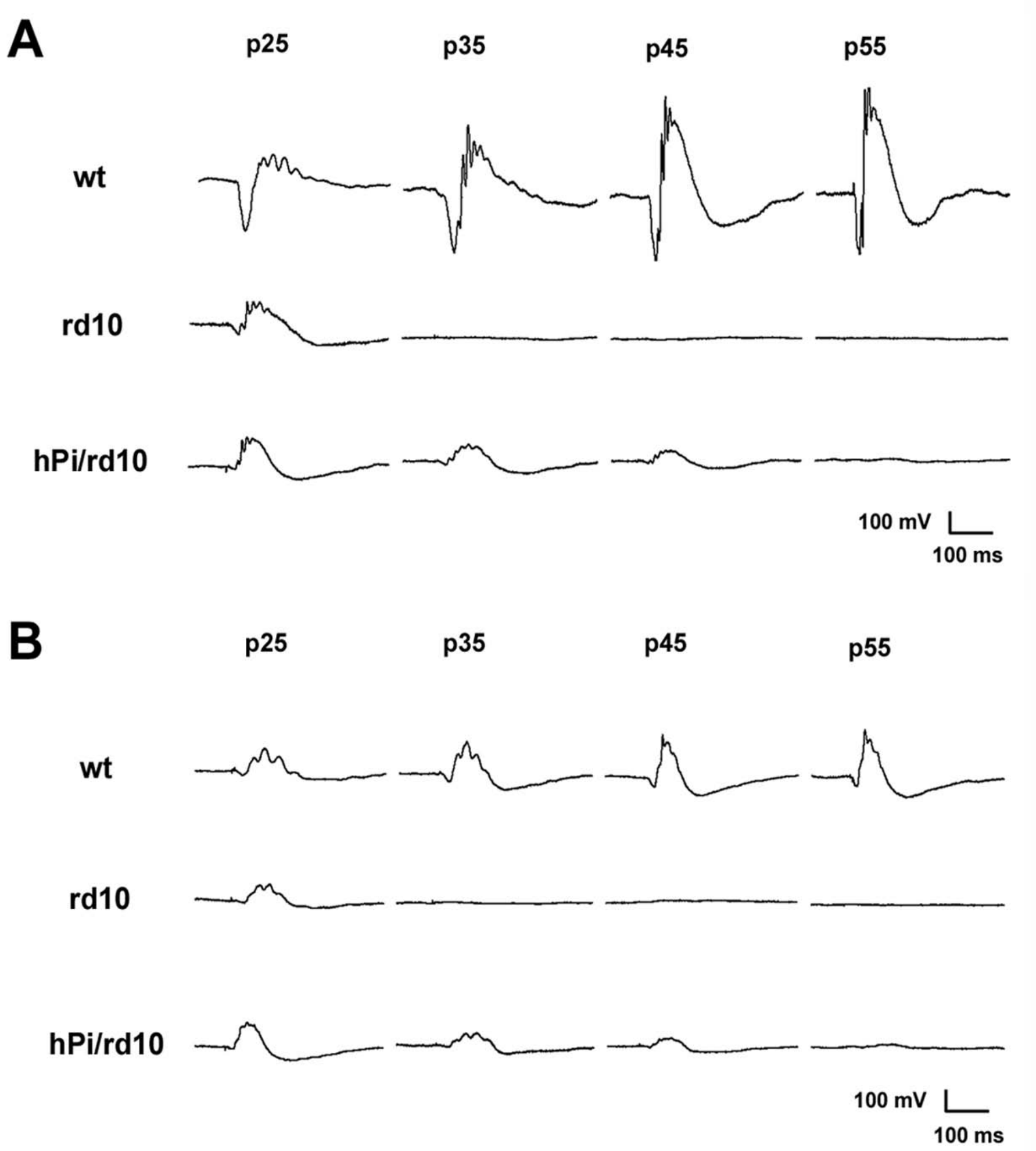
A
p25
p35
p45
p55
wt
rd10
hPi/rd10
100 mV
100 ms
B
p25
p35
p45
p55
wt
rd10
hPi/rd10
100 mV
100 ms